

## ECCENTRICITY OF MASING DISKS IN ACTIVE GALACTIC NUCLEI

PHILIP J. ARMITAGE<sup>1,2</sup>*ApJ, submitted*

## ABSTRACT

Observations of Keplerian disks of masers in NGC 4258 and other Seyfert galaxies can be used to obtain geometric distance estimates and derive the Hubble constant. The ultimate precision of such measurements could be limited by uncertainties in the disk geometry. Using a time-dependent linear theory model, we study the evolution of a thin initially eccentric disk under conditions appropriate to sub-pc scales in Active Galactic Nuclei. The evolution is controlled by a combination of differential precession driven by the disk potential and propagating eccentricity waves that are damped by viscosity. A simple estimate yields a circularization timescale of  $\tau_{\text{circ}} \sim 10^7 (r/0.1 \text{ pc})^{5/6} \text{ yr}$ . Numerical solutions for the eccentricity evolution confirm that damping commences on this timescale, but show that the subsequent decay rate of the eccentricity depends upon the uncertain strength of viscous damping of eccentricity. If eccentricity waves are important further decay of the eccentricity can be slow, with full circularization requiring up to 50 Myr for disks at radii of 0.1 pc to 0.2 pc. Observationally, this implies that it is plausible that enough time has elapsed for the eccentricity of masing disks to have been substantially damped, but that it may not be justified to assume vanishing eccentricity. We predict that during the damping phase the pericenter of the eccentric orbits describes a moderately tightly wound spiral with radius.

*Subject headings:* accretion, accretion disks — masers — galaxies: active — galaxies: Seyfert — galaxies: distances and redshifts — galaxies: individual (NGC 4258)

## 1. INTRODUCTION

Observations of water maser emission from a geometrically thin disk within the central pc of NGC 4258 (Miyoshi et al. 1995) have permitted a geometric determination of the distance to the galaxy (Herrnstein et al. 1999; Humphreys et al. 2008), and an estimate of the Hubble constant. The recent discovery of apparently similar maser emission in a number of more distant galaxies has raised the exciting prospect of a percent level determination of  $H_0$  independent of both distance ladder uncertainties and other cosmological parameters. Such a determination would have considerable cosmological utility, perhaps most importantly by improving the ability of current and future datasets to constrain the behavior of dark energy (Hu 2005; Olling 2007).

The precision with which  $H_0$  can be determined from measurements of masers in a single system is limited by uncertainties in the galactic peculiar velocity, observational errors, and any unmodeled complexity in the geometry of the source. The first two of these limits present instrumental and observational challenges, and considerable progress is guaranteed given sensitive, multi-epoch observations of maser disks at higher redshift than the one in NGC 4258. The third requires both observations and theory. Typically, it is assumed that the maser emission originates from a thin, circular disk, and this simplest assumption is consistent with all existing data on NGC 4258 (Humphreys et al. 2008). There is no obvious theoretical rationale, however, for assuming that the eccentricity is exactly zero, or for extrapolating the NGC 4258 results to other systems. Indeed, the obser-

vation that the masing disk in NGC 4258 is measurably warped suggests the possibility that different disks might exhibit a range of geometries. Although the geometry can be constrained observationally, this requires the introduction of additional parameters whose fitting inevitably degrades the precision with which the distance can be measured.

The purpose of this paper is to outline, from a theoretical perspective, the expected evolution of the eccentricity of a geometrically thin accretion disk at sub-pc distances from a supermassive black hole. Using a time-dependent linear theory model of an eccentric disk (Goodchild & Ogilvie 2006) I examine both the rate at which eccentricity decays, and the transient structure of the eccentric disk before it becomes circular.

## 2. DESCRIPTION OF THE DISK EVOLUTION

Consider a thin, flat disk in which the vertical scale height  $h \ll r$ . We define a complex eccentricity via,

$$E \equiv e \exp[i\varpi], \quad (1)$$

where  $e$  is the magnitude of the eccentricity and  $\varpi$  the longitude of pericenter of the fluid streamlines. We assume that at the radii of interest the potential is dominated by the Keplerian potential of the black hole  $\Phi_{\text{BH}}$ , to which must be added an additional contribution due to the disk,

$$\Phi = \Phi_{\text{BH}} + \Phi_{\text{disk}}. \quad (2)$$

The fluid in the disk has density  $\rho$ , pressure  $p$ , angular velocity  $\Omega$  and adiabatic exponent  $\gamma$ . We assume that turbulent stresses within the disk act to damp eccentricity, and parameterize the efficiency of the damping via a bulk viscosity  $\alpha_e$  written in terms of a Shakura-Sunyaev (1973)  $\alpha$  parameter. Linearization of the two-dimensional fluid equations (in the inviscid limit, except

<sup>1</sup> JILA, Campus Box 440, University of Colorado, Boulder CO 80309; pja@jilau1.colorado.edu

<sup>2</sup> Department of Astrophysical and Planetary Sciences, University of Colorado, Boulder CO 80309

for the aforementioned bulk viscosity) yields an evolution equation for the eccentricity (Goodchild & Ogilvie 2006),

$$2r\Omega \frac{\partial E}{\partial t} = -\frac{iE}{r} \frac{\partial}{\partial r} \left( r^2 \frac{d\Phi_{\text{disk}}}{dr} \right) + \frac{iE}{\rho} \frac{\partial p}{\partial r} + \frac{i}{r^2 \rho} \frac{\partial}{\partial r} \left[ (\gamma - i\alpha_e) pr^3 \frac{\partial E}{\partial r} \right]. \quad (3)$$

The first two terms on the right hand side describe precession driven by any non-Keplerian part of the disk potential and by pressure gradients within the disk. These terms do not change the magnitude of the eccentricity. The third term has the form of a Schrödinger equation – it describes waves of eccentricity that propagate radially through the disk and are damped by the action of viscosity.

Theoretically, it is expected that accretion disks in Active Galactic Nuclei (AGN) ought to be self-gravitating at the relatively large radii where masing occurs, and this permits some simplification of the evolution equation. We write the surface density as a power-law in radius,

$$\Sigma = \Sigma_0 r^\beta \quad (4)$$

and compute the disk potential  $\Phi_{\text{disk}}$  from the enclosed disk mass

$$M_{\text{disk}} = \int^r 2\pi r \Sigma dr \quad (5)$$

assuming a spherically symmetric mass distribution. We assume that over the relatively narrow radial range for which masing occurs the sound speed  $c_s$  can be taken (approximately) to be constant, and note that  $\rho \simeq \Sigma/2h$  and that  $h = c_s/\Omega$ . The rate of precession due to pressure gradients is then  $\propto c_s^2$  (a constant at the radii where masing occurs), while the rate of precession due to the non-Keplerian potential is  $\propto \Sigma_0$ , which rises with the disk mass<sup>3</sup>. Their ratio,

$$\frac{|\dot{E}_p|}{|\dot{E}_{\text{grav}}|} \sim \left( \frac{h}{r} \right)^2 \frac{M_{\text{BH}}}{M_{\text{disk}}} \quad (6)$$

therefore depends upon the disk mass – in low mass disks precession will be dominated by the pressure term while in higher mass disks gravity will dominate. The latter limit is probably appropriate for masing disks. At the radii – of the order of a tenth of a pc – where the masing is observed it is likely that disks around supermassive black holes are self-gravitating (Kolychalov & Sunyaev 1980; Clarke 1988; Shlosman, Begelman & Frank 1990; Goodman 2003). Self-gravitating disks develop spiral structure, whose existence in the NCG 4258 disk is hinted at by observations of clustering and asymmetry in the maser emission regions (Maoz 1995; Maoz & McKee 1998). For a self-gravitating disk  $M_{\text{BH}}/M_{\text{disk}} \approx (h/r)^{-1}$ ,  $|\dot{E}_p|/|\dot{E}_{\text{grav}}| \sim h/r$ , and pressure effects are negligible.

<sup>3</sup> These terms have different signs, so it is possible to choose a surface density and sound speed profile for which they cancel, or for which the disk precesses as a rigid body. Indeed, Statler (2001) derived a family of potentially long-lived eccentric disk models which owe their stability to rigid body precession. We do not consider special solutions of this type here, since there is no reason to expect that masing disks would have a structure that leads to vanishing differential precession.

Writing  $p = \rho c_s^2$  the evolution equation (3) then simplifies to,

$$2r\Omega \frac{\partial E}{\partial t} = 2\pi(\beta + 1)G\Sigma_0 r^\beta iE + \frac{ic_s^2}{r^2 \rho} \frac{\partial}{\partial r} \left[ (\gamma - i\alpha_e) \rho r^3 \frac{\partial E}{\partial r} \right]. \quad (7)$$

We study the eccentricity evolution implied by this equation in §3.

### 2.1. Limitations of this description

Equation (3) is an extremely simple representation of the evolution of an eccentric fluid disk. The most obvious limitation is the use of a linear equation rather than the nonlinear formalism developed by Ogilvie (2001). The linear equation ought to provide an approximate description of the dynamics at late times, when the eccentricity is small, but will evidently fail if the initial eccentricity and / or its variation with radius is large. A second and even more important limitation concerns the uncertain nature of the eccentricity damping. We have parameterized the damping via a bulk viscosity – rather than the usual shear viscosity used in the Shakura-Sunyaev theory of accretion disks – because disks dominated by a Navier-Stokes shear viscosity are unstable to *growth* of eccentric modes (Kato 1983; Ogilvie 2001). This is probably not a physical problem, rather it reflects the fact that angular momentum transport mediated by the magnetorotational instability (Balbus & Hawley 1998), self-gravity, or other physical mechanisms cannot be well described via a Navier-Stokes shear viscosity. For our purposes we simply assume that the stress in the disk acts such as to damp eccentricity, parameterize that damping efficiency (arbitrarily) via a bulk viscosity, and treat  $\alpha_e$  as a free parameter.

## 3. ECCENTRICITY EVOLUTION

### 3.1. Analytic estimates

The terms in equations (3) and (7) describing precession do not alter the magnitude of the disk eccentricity. The wave-like term proportional to  $\gamma$  *does* change the local eccentricity, but preserves a global invariant (Goodchild & Ogilvie 2006),

$$\mathcal{E}^2 \equiv \int_{r_{\text{in}}}^{r_{\text{out}}} \frac{1}{2} r^3 \rho \Omega |E|^2 dr. \quad (8)$$

Damping of  $\mathcal{E}^2$  occurs due to the viscous term at a rate

$$\frac{d\mathcal{E}^2}{dt} = - \int_{r_{\text{in}}}^{r_{\text{out}}} \frac{1}{2} \alpha_e pr^3 \left| \frac{\partial E}{\partial r} \right|^2 dr. \quad (9)$$

The presence of eccentricity waves means that the radial profile of  $E$  needs to be considered along with the temporal evolution. This requires a numerical solution of equation (7), which we defer to §3.2. For an estimate, however, we can define a local damping timescale,

$$\tau_{\text{damp}} = \frac{\rho \Omega |E|^2}{\alpha_e p |\partial E / \partial r|^2}, \quad (10)$$

which is simply the ratio of the right hand sides of equations (8) and (9). If  $E$  varies on the same scale as the azimuthally averaged disk properties then to order of magnitude  $|\partial E / \partial r|^2 \simeq E^2 / r^2$  and we find that,

$$\tau_{\text{damp}} = \frac{1}{\alpha_e \Omega} \left( \frac{h}{r} \right)^{-2}. \quad (11)$$

This is just the usual “viscous time” of the disk if  $\alpha_e$ , the viscosity responsible for damping eccentricity, is comparable to the shear viscosity  $\alpha_s$  driving mass inflow<sup>4</sup>. It is well known that, at radii of 0.1 pc and beyond, the viscous time in AGN disks is extremely long (Shlosman, Begelman & Frank 1990). For the specific case of NGC 4258, observations of the thickness of the masing disk imply a midplane temperature of  $T \simeq 600$  K and a sound speed  $c_s \simeq 1.5 \text{ kms}^{-1}$  (Argon et al. 2007), consistent with the conditions needed for H<sub>2</sub>O maser emission. Adopting these values, the viscous time is

$$\tau_{\text{visc}} = 5.7 \times 10^8 \left( \frac{\alpha_s}{0.1} \right)^{-1} \left( \frac{c_s}{1.5 \text{ kms}^{-1}} \right)^{-2} \times \left( \frac{M_{\text{BH}}}{4 \times 10^7 \text{ yr}} \right)^{1/2} \left( \frac{r}{0.1 \text{ pc}} \right)^{1/2} \text{ yr}. \quad (12)$$

Unless sub-pc disks in AGN remain unperturbed across timescales of the order of a Gyr, circularization *due to viscous evolution* will not occur.

Much faster circularization occurs as an indirect consequence of differential precession, which for the disks of interest is of the order of  $(h/r)^{-1} \sim 10^3$  times faster than viscous evolution. The precession timescale  $\tau_p = 2\pi/\omega$ , where

$$\omega = -\frac{1}{2r^2\Omega} \frac{d}{dr} \left( r^2 \frac{d\Phi_{\text{disk}}}{dr} \right). \quad (13)$$

As noted above, we expect disks at radii of the order of 0.1 pc around AGN to be self-gravitating, in which case (Toomre 1964)

$$Q \equiv \frac{c_s \Omega}{\pi G \Sigma} \sim 1 \quad (14)$$

where  $\Sigma$  is the disk surface density. Using this relation to fix the surface density in terms of the sound speed (assumed constant) and disk radius, we find,

$$\tau_p = 8.2 \times 10^5 Q \left( \frac{c_s}{1.5 \text{ kms}^{-1}} \right)^{-1} \left( \frac{r}{0.1 \text{ pc}} \right) \text{ yr}, \quad (15)$$

independent of the black hole mass. This relatively rapid precession has an important consequence. Although it does not alter  $e$ , the differential precession leads to a rapid variation of  $\varpi$  with radius. This reduces the characteristic lengthscale over with  $E$  varies in equation (10), and allows viscosity to damp the eccentricity much more quickly.

The origin of the gas in the masing disks of Seyfert galaxies is not known. One possibility is that the disk is established following the infall of relatively small amounts of low angular momentum gas (King & Pringle 2007). In this scenario, one expects the disk to be initially non-circular, with the fluid streamlines describing nested aligned ellipses. Partially motivated by such a picture, we consider as initial conditions a disk in which  $e \neq 0$  and  $\varpi = \text{const}$ . After time  $t$ , the pericenters of ellipses separated by radial distance  $\Delta r$  have angular separation,

$$\Delta\varpi = \frac{d\omega}{dr} \Delta r t. \quad (16)$$

<sup>4</sup> This argument leads to the rule of thumb that an eccentric disk ought to circularize “on the viscous timescale”. This is potentially misleading, first because there is no direct physical relation between  $\alpha_e$  and  $\alpha_s$ , and, second, because differential precession can lead to a situation in which  $|\partial E / \partial r|^2 \gg E^2 / r^2$  in much less than a viscous time, allowing for faster eccentricity evolution.

Defining the winding scale as the radial separation for which  $\Delta\varpi = 2\pi$ ,

$$\Delta r_{\text{wind}} = \frac{4\pi Q}{c_s} \frac{r^2}{t}. \quad (17)$$

This scale decreases inversely with  $t$ , and as a result the timescale on which viscosity can damp the eccentricity (equation 10) scales with the system age as,

$$\tau_{\text{damp}} = \frac{\Omega}{\alpha_e c_s^2} \left( \frac{4\pi Q}{c_s} \right)^2 \frac{r^4}{t^2}. \quad (18)$$

The disk will circularize when  $t \sim \tau_{\text{damp}}$ . Defining this time as the circularization time  $\tau_{\text{circ}}$ , we obtain,

$$\tau_{\text{circ}} = (4\pi Q)^{2/3} (GM_{\text{BH}})^{1/6} \alpha_e^{-1/3} c_s^{-4/3} r^{5/6}, \quad (19)$$

which displays only a weak dependence on the black hole mass and on the (very uncertain) viscosity damping the eccentricity. Since masing action is only possible over a fairly limited range of disk temperatures the only significant dependence is the almost linear scaling of the circularization timescale with radius. Adopting representative values of the parameters the timescale is,

$$\tau_{\text{circ}} = 8.5 \times 10^6 Q^{2/3} \left( \frac{M_{\text{BH}}}{10^8 M_\odot} \right)^{1/6} \left( \frac{\alpha_e}{0.1} \right)^{-1/3} \times \left( \frac{c_s}{1.5 \text{ kms}^{-1}} \right)^{-4/3} \left( \frac{r}{0.1 \text{ pc}} \right)^{5/6} \text{ yr}. \quad (20)$$

This simple calculation provides an estimate of when enough differential precession will have accumulated to start eccentricity damping. If *only* differential precession and damping are considered then subsequent evolution will simply wrap up the eccentricity vector into an ever-tighter spiral, hastening the decay of  $\mathcal{E}^2$  even further. Indeed, very rapid damping due to this process was seen in numerical solutions for precessing *warped* disks in the regime where the warp is transmitted viscously (Armitage & Natarajan 1999). In the eccentric case, however, inspection of equation (7), shows that once damping is important (or even beforehand), the wavelike term proportional to  $\gamma$  is also likely to be significant. This term can offset differential precession, and affect the rate at which further decay of the eccentricity occurs. As we show subsequently, it turns out that while equation (20) suffices to predict the onset of eccentricity damping fairly accurately, the rate of subsequent decay varies with  $\alpha_e$  much more strongly than would be suspected based on the rather weak scaling derived above.

### 3.2. Numerical results

To study the eccentricity evolution in more detail we have computed numerical solutions to equation (7). We discretize the equation on a uniform spatial grid between  $r_{\text{in}}$  and  $r_{\text{out}}$ , and advance the system in time using a second-order scheme that, in the absence of damping, preserves the invariant  $\mathcal{E}^2$  to sufficient accuracy for our purposes. We assume that the inner disk is circular, and set  $E = 0$  at the inner boundary  $r_{\text{in}}$ . The correct boundary conditions to apply at  $r_{\text{out}}$  are less clear, since the outer edge of the masing region may reflect either a physical disk edge (defined, for example, by the onset of disk fragmentation) or merely the

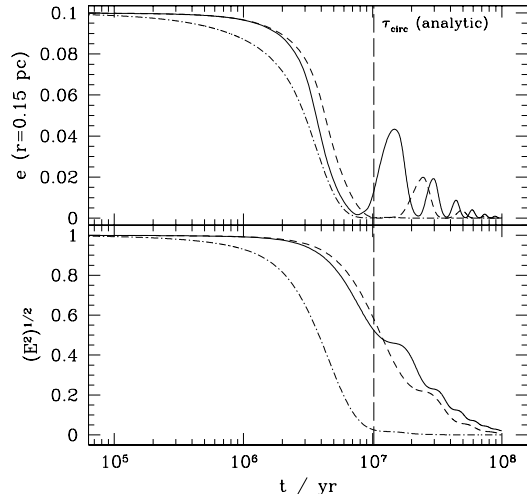


FIG. 1.— The evolution of the eccentricity at  $r = 0.15$  pc (upper panel) and eccentricity invariant  $(\mathcal{E}^2)^{1/2}$  (lower panel) computed from numerical solutions to equation (7). The units on the vertical axes are arbitrary. Three runs are shown, all of which assume a  $Q = 1$  disk around a black hole of mass  $4 \times 10^7 M_\odot$ . The disk has a constant sound speed of  $1.5$  km/s and  $\gamma = 1.4$ . The initial eccentricity is a gaussian centered on  $0.15$  pc with a width of  $0.05$  pc and a constant  $\varpi$ . The solid curves show results for a disk extending from  $0.05$  pc to  $0.4$  pc, with  $\alpha_e = 0.1$ . The dashed curves depict the evolution of an identical disk within larger boundaries that extend from  $0.025$  pc to  $0.8$  pc. The vertical dashed line shows the analytic estimate for the circularization time for these parameters. The dot-dashed curves show the effect of increasing the damping coefficient to  $\alpha_e = 1$ .

outer extent of the zone that produces maser emission (Neufeld, Maloney & Conger 1994). Typically we use zero-gradient conditions on the components of  $E$  (i.e.  $\partial E_x / \partial r = \partial E_y / \partial r = 0$  at  $r_{\text{out}}$ ). We have run models with different boundary conditions, and with different choices for  $r_{\text{out}}$ , to gauge the effect of the boundaries on the results.

Figure 1 shows the decay of an initially gaussian eccentricity perturbation,

$$e(r) = e_0 \exp \left[ -\frac{(r - r_0)^2}{\Delta r^2} \right] \\ \varpi(r) = 0 \quad (21)$$

centered on  $r_0 = 0.15$  pc with width  $\Delta r = 0.05$  pc. As this is a linear calculation, the value of  $e_0$  is entirely arbitrary. We assume a  $Q = 1$  disk with a constant sound speed  $c_s = 1.5$  km/s, which results in a  $\Sigma \propto r^{-3/2}$  surface density profile. The black hole mass is set to the NGC 4258 value of  $4 \times 10^7 M_\odot$ . The Figure shows results obtained from two models with  $\alpha_e = 0.1$  (which differ only in the radial extent of the disk), and one model with stronger eccentricity damping  $\alpha_e = 1$ . We plot both the eccentricity of the disk at  $r_0$ , and the integrated eccentricity invariant  $\sqrt{\mathcal{E}^2}$  in a form that is proportional to the magnitude of the eccentricity.

The numerical results confirm that the analytic estimate of the damping timescale (equation 20) is reasonably accurate. For the two runs with  $\alpha_e = 0.1$  we find that  $\sqrt{\mathcal{E}^2}$  drops by a factor of two after  $10$  Myr of evolution, as predicted. For these runs, however, subse-

quent damping is relatively slow. It takes approximately  $50$  Myr for  $\sqrt{\mathcal{E}^2}$  to decay from its initial value by an order of magnitude. The corresponding curve showing the local value of  $e$  displays clearly the wave-like nature of the evolution. Although  $e$  displays a general decaying trend the evolution is oscillatory rather than a monotonic decline, with the period of the oscillations varying with the radial extent of the disk. Only for strong damping ( $\alpha_e \approx 1$ ) is the wave-like behavior suppressed. In the strong damping limit the initial decay of the eccentricity is not that much faster than in the weakly damped cases but, once damping has set in, the subsequent decline of the eccentricity to negligible values is rapid.

We have also studied the effect of different initial conditions. In general, we find that the decay rate of  $\sqrt{\mathcal{E}^2}$  is quite robust against changes in the initial conditions. The evolution of the value of  $e$  at a particular radius, on the other hand, can exhibit large transients at relatively early times if the initial conditions contain large gradients in  $E$ . Physically it seems likely that an eccentric disk would settle down to a smooth distribution of  $E$  shortly after formation, so the gaussian initial conditions we have plotted ought to be representative of the likely evolution.

Figure 2 plots the spiral traced by  $\varpi(r)$  at different times in the weakly damped run ( $\alpha_e = 0.1$ ) with the smaller radial extent of the disk ( $0.05 \text{ pc} < r < 0.4 \text{ pc}$ ). The initial evolution of the eccentricity vector is driven by differential precession, with damping setting in once the spiral has become sufficiently tightly wound – for this run a value of  $r d\varpi/dr \simeq 2\pi$ , which is achieved after a few Myr, suffices. During the damping phase there is no further increase in the winding due to differential precession, which is offset by the wave-like term in the evolution equation. As a consequence, final damping of the eccentricity in the low  $\alpha_e$  runs occurs relatively slowly. Indeed, as shown in Figure 3, for the low  $\alpha_e$  runs the sense of the spiral pattern *reverses* during the damping phase roughly periodically, though only the first of these reversals is likely to have any physical significance since at later times the actual magnitude of the eccentricity is quite small. As with the eccentricity oscillations described above, the reversals are largely eliminated in the more strongly damped run.

Based on the above results, it is clear that while the eccentricity is decaying the structure of the disk can be complex. It is not even possible to predict securely whether the eccentricity vector will describe a leading or a trailing spiral pattern. At almost all epochs a description of the disk in terms of aligned nested ellipses is a very poor approximation. A better description is to assume a linear radial variation in  $\varpi$ ,

$$\varpi(r) = \varpi(r_0) + \left( \frac{d\varpi}{dr} \right)_{r_0} (r - r_0). \quad (22)$$

As shown in Figure 2, this description is usually reliable over at least a factor of two in radius. Typical values of the twist in the eccentricity vector,  $r d\varpi/dr$  are in the range of  $\pi$  to  $2\pi$ . We believe that fitting a model of this kind to observational data would represent a substantial improvement over a model with  $\varpi = \text{const}$ , though at the cost of introducing an additional free parameter in the winding angle of the eccentricity vector.

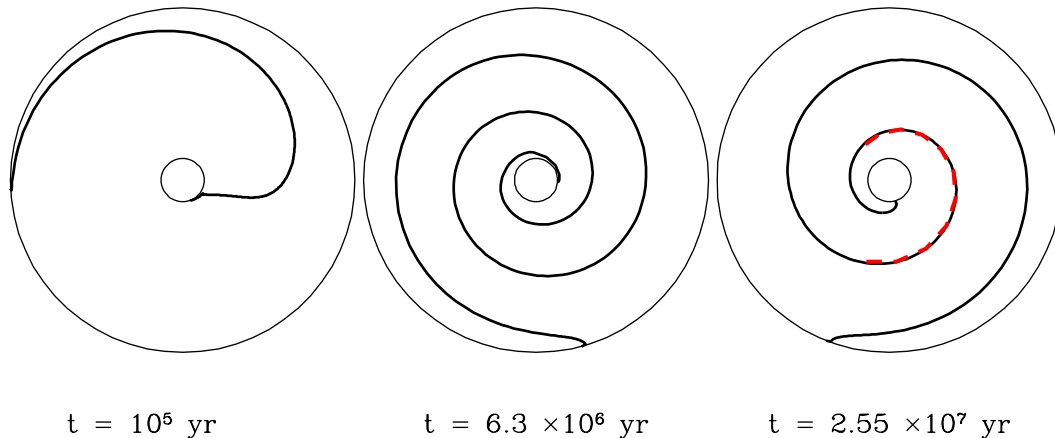


FIG. 2.— The radial variation of the angle of pericenter  $\varpi$  of the fluid streamlines, plotted at different times. The run corresponds to the solid curves in Fig. 1. The eccentricity vector is wound up by differential precession until damping sets in. As waves subsequently propagate through the disk the spiral pattern periodically reverses, as shown in the rightmost panel. The heavy dashed curve in the rightmost panel shows a linear fit to  $\varpi(r)$ , which is reasonably accurate at most epochs over a limited range (a factor of two) in radius.

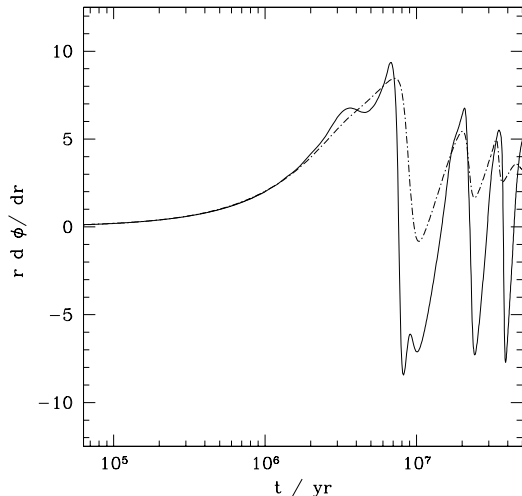


FIG. 3.— The evolution of the twist  $r d\varpi/dr$  in the eccentricity vector, evaluated at  $r = 0.15$  pc for the standard run (solid curve, with parameters corresponding to the same curve in Fig. 1) and the run with  $\alpha_e = 1$ . The weakly damped case displays approximately periodic reversals between leading and trailing spiral patterns in the eccentricity vector. These occur on a timescale of the order of  $10^7$  yr. The oscillations are largely suppressed in the run with stronger eccentricity damping.

#### 4. DISCUSSION

Theory provides scant guidance as to the formation mechanism and lifetime of sub-pc disks in AGN. The long viscous timescale at these radii – of the order of a Gyr – means that it is unlikely that such disks formed from outward viscous expansion of gas that was initially much closer to the black hole, but this still leaves several possibilities for feeding gas directly to sub-pc radii. One idea is that clouds on low angular momentum orbits are sporadically shredded by the tidal field of the black hole, with the debris cooling and settling into a

disk (King & Pringle 2007). Depending upon the disk mass and radius involved, the result could be a stable gaseous disk or gravitational fragmentation into a disk of stars (Gammie 2001; Rice et al. 2003). Such an idea provides one possible explanation for the disk of young stars observed at sub-pc radii from our own Galactic Center (Levin & Beloborodov 2003). If this is the origin of the masing disks then it is probable that the initial conditions would involve eccentric and / or warped disks. However, there are also plausible scenarios that would yield initially circular disks. For M31, for example, it has been suggested that the innermost, circular, disk of stars formed from a gravitationally unstable disk that accumulated from the stellar winds of stars situated further out (Chang et al. 2007). Given these very different models, the observation that the masing disk in NGC 4258 is at least approximately circular (Humphreys et al. 2008) raises two questions. First, does the lack of obvious eccentricity constrain the formation mechanism to favor the scenarios that yield initially circular orbits? Second, it is reasonable to assume that the (unmeasured) eccentricity is actually vanishingly small? In this paper we have attempted to provide partial answers to both of these questions.

Our main result is that the *initial* damping of a thin self-gravitating disk at sub-pc distances from a black hole is relatively rapid. The timescale at 0.1 pc is around 10 Myr, and even this may be an overestimate since any nonlinear effects (such as the formation of shocks as elliptical orbits precess) will hasten the decay further. Rapid damping is driven by differential precession, which occurs on a much shorter timescale than the viscous evolution of the disk. The lack of gross eccentricity in NGC 4258 is therefore not surprising, and does not constrain the disk formation mechanism. Once damping is underway, however, it can take a surprisingly long period for the eccentricity to decay to negligible levels. If the viscous coefficient governing eccentricity damping is relatively small ( $\alpha_e = 0.1$  in our description) the presence of waves in

the disk allows significant eccentricity to survive for up to 50 Myr. Evidently it would be useful to *determine* the efficiency of eccentricity damping under the conditions likely to prevail at sub-pc radii, perhaps via improved simulations of self-gravitating eccentric disks, which to date have focused on simpler questions such as whether the disk fragments or not (Alexander et al. 2008). Currently, though, it seems unwise to conclude that a good upper limit on the eccentricity implies strictly circular orbits.

Finally, we addressed the question of the predicted orbital structure of an eccentric disk during the circularization process. Existing constraints on the eccentricity of the NGC 4258 disk (Humphreys et al. 2008) have been derived assuming a model, developed by Statler (2001) for different purposes, in which the eccentric orbits are

aligned and nested. In the case of very thin masing disks this model is not a good approximation to the likely structure, which instead involves a moderately tightly wound spiral in the angle of periaapse. A reasonable fit, over a modest range of radii, is possible using the next order approximation in which the periaapse angle is a linear function of orbital radius.

This work was stimulated by discussions with Fred Lo, and completed at the urging of Dick McCray, to whom I am indebted. My research was supported by NASA under grants NNG04GL01G and NNX07AH08G from the Astrophysics Theory Programs, and by the NSF under grant AST 0407040.

#### REFERENCES

- Alexander, R. D., Armitage, P. J., Cuadra, J., & Begelman, M. C. 2008, *ApJ*, in press (arXiv:0711.0759v1)
- Argon, A. L., Greenhill, L. J., Reid, M. J., Moran, J. M., & Humphreys, E. M. L. 2007, *ApJ*, 659, 1040
- Armitage, P. J., & Natarajan, P. 1999, *ApJ*, 525, 909
- Balbus, S. A., & Hawley, J. F. 1998, *Reviews of Modern Physics*, 70, 1
- Chang, P., Murray-Clay, R., Chiang, E., & Quataert, E. 2007, *ApJ*, 668, 236
- Clarke, C. J. 1988, *MNRAS*, 235, 881
- Elitzur, M., Hollenbach, D. J., & McKee, C. F. 1989, *ApJ*, 346, 983
- Gammie, C. F. 2001, *ApJ*, 553, 174
- Goodchild, S., & Ogilvie, G. 2006, *MNRAS*, 368, 1123
- Goodman, J. 2003, *MNRAS*, 339, 937
- Herrnstein, J. R., Moran, J. M., Greenhill, L. J., Diamond, P. J., Inoue, M., Nakai, N., Miyoshi, M., Henkel, C., & Riess, A. 1999, *Nature*, 400, 539
- Hu, W. 2005, in *Observing Dark Energy*, eds S. C. Wolff & T. R. Lauer, ASP Conference Series, Vol. 339, ASP (San Francisco), p. 215 (arXiv:astro-ph/0407158v1)
- Humphreys, E. M. L., Reid, M. J., Greenhill, L. J., Moran, J. M., & Argon, A. L. 2008, *ApJ*, 672, 800
- Kato, S. 1983, *PASJ*, 35, 249
- King, A. R., & Pringle, J. E. 2007, *MNRAS*, 377, L25
- Levin, Y., & Beloborodov, A. M. 2003, *ApJ*, 590, L33
- Kolychalov, P. I., & Sunyaev, R. A. 1980, *Soviet Astronomy Letters*, 6, 357
- Maoz, E. 1995, *ApJ*, 455, L131
- Maoz, E., & McKee, C. F. 1998, *ApJ*, 494, 218
- Miyoshi, M., Moran, J., Herrnstein, J., Greenhill, L., Nakai, N., Diamond, P., & Inoue, M. 1999, *Nature*, 373, 127
- Neufeld, D. A., Maloney, P. R., & Conger, S. 1994, *ApJ*, 436, L127
- Ogilvie, G. I. 2001, *MNRAS*, 325, 231
- Olling, R. P. 2007, *MNRAS*, 378, 1385
- Rice, W. K. M., Armitage, P. J., Bate, M. R., & Bonnell, I. A. 2003, *MNRAS*, 339, 1025
- Shakura, N. I., & Sunyaev, R. A. 1973, *A&A*, 24, 337
- Shlosman, I., Begelman, M. C., & Frank, J. 1990, *Nature*, 345, 679
- Statler, T. S. 2001, *AJ*, 122, 2257
- Toomre, A. 1964, *ApJ*, 139, 1217